Practical Considerations for Understanding Surface Reaction Mechanisms Involved in Heterogeneous Catalysis

Daniyal Kiani* and Israel E. Wachs*

Read Online

ACCESS | Metrics & More | Article Recommendations | Supporting Information

ABSTRACT: Acquiring useful knowledge about the active site(s) of a catalyst, nature of reactant−catalyst interactions, nature of reactive intermediates, rate-determining step, reaction rate orders that affect various process parameters, and reaction mechanism as a whole is exceedingly challenging. This is especially true in the case of heterogeneous catalysts due to the complexity of the nature of surface active sites and their nonstatic behavior. Here, we present our perspective on differentiating between various surface reaction mechanisms in light of pioneering studies by leaders in the field, with the aim of clarifying some of the confusion associated with these complex mechanisms, especially the Eley−Rideal mechanism. Using bibliometric analysis, we identify and discuss the following four reactions that most commonly invoke the Eley−

Rideal mechanism: H_2 activation, CO oxidation, esterification of alcohols by acids, and selective catalytic reduction (SCR) of NO_x with NH_3. Our analysis of studies utilizing well-suited experimental and computational methodologies for differentiating surface reaction mechanisms suggests that the above-mentioned four reactions do not occur via the Eley−Rideal mechanism. Instead, each reaction occurs via the Langmuir−Hinshelwood mechanism with nonidealities present. Lastly, we highlight practical considerations regarding select experimental (characterization methods and differential kinetics) and computational modeling that we believe can provide useful insights to accurately discern between the various possible reaction mechanisms in heterogeneous catalysis.

KEYWORDS: *surface science, differential kinetics, molecular beam spectroscopy, scanning tunneling spectroscopy, isotope-switches*
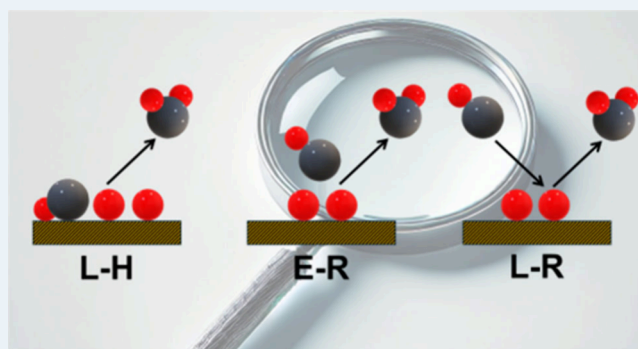
1. INTRODUCTION

In 1922, Langmuir postulated that surface-catalyzed reactions could occur via the following three distinct reaction mechanisms:[1−3]

   i. A reaction between two adsorbed molecules. It is generally understood that both reacting molecules have to be chemisorbed on adjacent catalyst sites in this case. Langmuir cited H_2 activation over tungsten filament as an example of a reaction where this mechanism prevails.[3]

   ii. A reaction between an adsorbed molecule and the underlying atoms of the catalyst itself. In the 1922 publication, Langmuir discussed H_2 oxidation over defect-rich CuO in the absence of gaseous O_2 as an example of this reaction mechanism.[3]

   iii. A reaction between an adsorbed molecule on the surface and a gas-phase molecule that does not undergo any sort of adsorption prior to the reaction. Langmuir identified CO oxidation (gaseous CO colliding with O* atoms) over Pt catalyst as an example of a reaction occurring via this mechanism.[3]

In subsequent years, the first reaction mechanism became known as the Langmuir−Hinshelwood mechanism (L-H), and a modified variant of this mechanism is also referred to as the

Langmuir−Hinshelwood−Hougon−Watson mechanism (L-H-H-W) in the chemical engineering community. The second reaction mechanism, often invoked in the alkane (especially methane) partial oxidation literature,[4−6] is now known as the Mars−van Krevelen (MvK) mechanism because Mars and van Krevelen provided the mathematical formalism describing the kinetics of this mechanism in 1954.[7] It is noteworthy, however, that Langmuir clearly outlined the idea of a solid catalyst providing oxygen species to oxidize an adsorbing reactant in the absence of gas-phase O_2 when he discussed H_2 oxidation on defect-rich CuO in 1922, three decades before Mars and van Krevelen discussed this mechanism.[3] We direct the reader to dedicated perspectives/reviews on the MvK mechanism[8,9] and will not further focus on MvK surface reaction mechanisms in the remainder of this Perspective. Although the third mechanism is now known as the Eley−Rideal (E-R) mechanism, we agree

with Prins[1] that it is more suitable to call it the Langmuir−Rideal mechanism (L-R) for the following two reasons: (i) Langmuir proposed this mechanism in 1922, well before papers by Eley and Rideal were published, and (ii) a mechanism where only a physisorbed species reacts with a chemisorbed species, which is distinct from the L-R mechanism, should be called the E-R mechanism.[1] As explained by Eley and Rideal in their studies in the 1930s and 1940s,[10,11] the mechanism they envisioned and later categorically described as "van der Waals−chemisorbed layer interaction, VCI," arguably constitutes a reaction between a physisorbed and a chemisorbed molecule and not a gas-phase species reacting with an adsorbed species, as Langmuir had postulated in his work in 1922. In the actual E-R mechanism, the physisorbed species was hypothesized to be in a relatively deep van der Waals trough above and between the constituents of the chemisorbed layer, at least by Rideal.[10] Accounting for the distinction between the L-R mechanism and the true E-R mechanism, there are actually four distinct surface reaction mechanisms operable in heterogeneous catalysis (L-H, MvK, L-R, and E-R).

The adsorbate−catalyst interactions involved in physisorption are long-range, as schematically depicted in Figure 1, and the electron density is separately redistributed within the adsorbate and catalyst.[9] Furthermore, there is a minuscule (often negligible) exchange of electrons, and the magnitude of the adsorption enthalpy (H_{ads}) is usually <35 kJ mol^{-1} for small adsorbates.[12] The characteristic lifetime of a physisorbed molecule on the surface before desorbing is often cited to be on the order of 10^{-13} s; however, this characteristic surface residence time remains contested and may vary by orders of magnitude depending on the temperature, adsorption energy, etc.[12] For instance, Ertl et al. suggested that the surface residence time for an adsorbate with an adsorption energy of 41.84 kJ mol^{-1} at 300 K would be 10^{-6} s, and if the reactant came directly from the gas phase or was adsorbed with a much lower adsorption energy, the surface residence time would be closer to the vibrational period of 10^{-13} s.[13] As a gaseous molecule physisorbs on a solid catalyst surface, the surface potential (i.e., overspill of electronic charge at the solid surface) results in an imbalance of the local electron density on either side of the gas−solid interface.[12] This small localized charge imbalance becomes more significant as the polarizability of the adsorbate increases, and thus, highly polarizable molecules will physisorb more strongly than weakly polarizable molecules.[12] For instance, a recent study showed that heavier adsorbates especially with heteroatoms (i.e., higher polarizability), for example thiophene, pyridine, etc., physisorbed on unreactive surfaces like the basal plane of MoS_2 can exhibit adsorption enthalpies in the 50−100 kJ mol^{-1} range.[14] Therefore, while physisorption entails weak interaction between an adsorbate and the adsorbent surface, it can be appreciable enough to prevent fully elastic scattering of molecules from the surface of the solid if a molecular beam of adsorbate impinges onto the solid catalyst (*vide infra*). Hence, we caution against overgeneralizing adsorption enthalpies and solely relying on adsorption enthalpy magnitudes to differentiate between physisorption and chemisorption.

Conversely, chemisorption entails significant electron exchange between the adsorbate and the adsorbent, leading to H_{ads} values higher than 35 kJ mol^{-1} due to short-range, strong adsorbate−catalyst interactions.[12] For common heterogeneous catalysts composed of transition metals and metal oxides, chemisorption occurs via the splitting of the original bonding and antibonding orbitals of the adsorbate into new levels, and
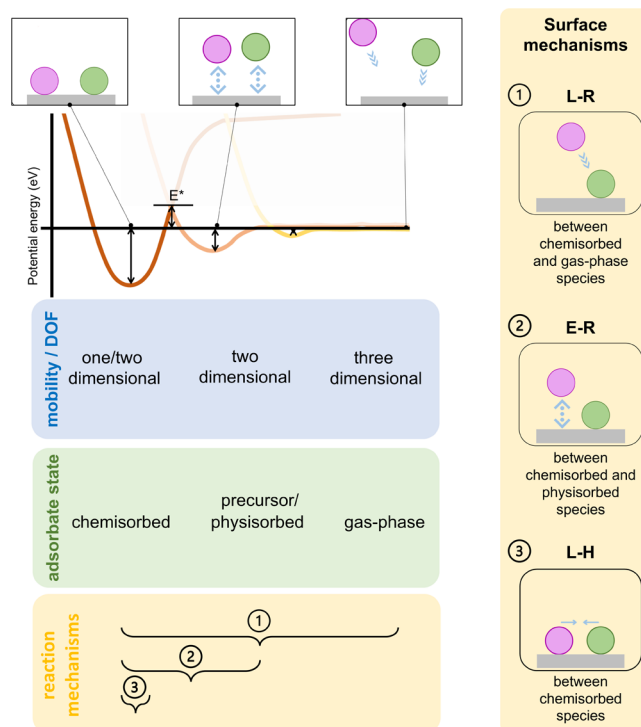

Figure 1. One-dimensional Lennard-Jones potential energy diagram for the approach of gaseous molecules from the gas phase to the surface of a solid catalyst. Depending on the depth of the potential energy well, the adsorption is described as a precursor state, physical or chemical in nature. The distinction is in fact qualitative because it reflects the type of interaction involved: weak van der Waals forces in physisorption and stronger covalent bonding in chemisorption.[10] Sometimes, physisorption that precedes chemisorption is referred to as the "precursor state" (i.e., precursor state and physisorption may describe the same species depending on the literature report being used). A precursor state represents a species that has thermally equilibrated with the catalyst surface, but its lifetime is significantly shorter than the lifetime of chemisorbed species.[15] The magnitude of the activation barrier (E^*) can vary, and it is >0 if chemisorption is activated, as in dissociative adsorption of molecular H_2 as 2H* on metal surfaces like Cu (100).[16] Mobility/degrees of freedom (DOF) decreases moving from the gas phase to physisorbed/precursor to chemisorbed states. Note that the fourth mechanism (MvK) is not shown in this figure, as it is discussed in dedicated reviews.[8,9] Hence, it is not the focus of our discussion and has been omitted for brevity.

electronic exchange occurs between these new levels and the empty d orbitals of the transition metal or metal oxide adsorption site. Moreover, in the case of chemisorption, the H_{ads} value also depends on the coverage of the adsorbate on the catalyst surface since lateral interactions between the adsorbed molecules usually come into play.[12]

Noting the differences between gas-phase, physisorbed, and chemisorbed molecules, it is clear that differences in reaction between a physisorbed molecule vs a gas-phase molecule with a chemisorbed molecule on the catalyst surface are not necessarily trivial and are generally expected to have profound implications for the reaction kinetics, entropic changes, and activation barrier of various steps in a catalytic reaction. In other words, the Gibbs free energy of a catalytic reaction, which is the sum of the enthalpic and entropic terms, is dependent on this minuscule yet critical detail regarding the initial reference state of the reactant molecule (i.e., freely moving in the gas phase vs laterally diffusing in a physisorbed state vs being immobile or mobile in a

chemisorbed state). Therefore, we make a case that more nuanced terminology could be used to differentiate the various reaction mechanisms, especially between the L-R and E-R mechanisms, that are currently typically collectively described by the E-R kinetic expression. We schematically highlight the difference between the L-H, L-R, and E-R reaction mechanisms in Figure 1.

In the majority of the heterogeneous catalysis literature, labeling of the true E-R mechanism by a blanket E-R descriptor that is loosely defined and encompasses both the L-R mechanism (chemisorbed species reacting with gas-phase species) and the true E-R mechanism (chemisorbed species reacting with physisorbed species) makes it challenging to understand the assumptions and dynamics of the underpinning surface reaction mechanism. In this Perspective, we aim to encourage researchers to consider these critical differences between E-R and L-R mechanisms and to strive to differentiate between the E-R and L-R mechanisms instead of applying the vague descriptor. Given the challenges of differentiating between various reaction mechanisms operable in heterogeneous catalysis, the importance of pertinent characterization and well-designed kinetic studies is clear. If the nature of the reactive species, the nature of the active sites, and the operable mechanism(s) are not fully understood at the time of the publication of a scientific report, we encourage authors to entertain all possibilities explicitly (e.g., both E-R and L-R) with the intent to guide future research efforts.

We conducted a literature analysis on the Web of Science database for the use of the term "Eley-Rideal" in all available publications. The titles of the papers using this term were further analyzed for key terms (minimum occurrence of keywords: 10) to ascertain different reactions within the broader heterogeneous catalysis literature that most often invoke the E-R mechanism. Out of the 4815 key terms identified, 113 terms were repeated at least 10 times, out of which the top/most relevant 68 terms were used to generate a network diagram using VOSviewer,[17] shown in the Supporting Information.

Based on the bibliometric analysis (Supporting Information), it is apparent that the E-R catalysis literature predominantly comprises four clusters of catalytic reactions where the E-R mechanism is most often invoked. The four catalytic reactions are

   i. Hydrogen activation (H-D exchange, *ortho-* to *para*-hydrogen conversion, hydrogenation, etc.), typically over Pt-group metal (PGM) catalysts.

   ii. CO oxidation (over PGM catalysts and more recently over single-atom catalysts).

   iii. Esterification (including transesterification) of alcohols by solid oxide acid catalysts.

   iv. Selective catalytic reduction (SCR) of NO_x with NH_3 (typically over Cu-SSZ-13 and V_2O_5-WO_3/TiO_2 catalysts).

The literature was next analyzed for the co-occurrence of the terms "*in situ*" or "*operando*" with "Eley-Rideal", and 296 reports met this search criteria. These reports were further analyzed with a bibliometric network to identify key terms to gain insight into which reaction classes were reporting *in situ* or *operando* spectroscopic evidence among the reaction classes that invoke the E-R mechanism most often. From the bibliometric network analysis shown in the Supporting Information, it is apparent that the reports predominantly related to the NH_3 SCR reaction invoking the E-R mechanism are the ones that at least also

contain some *in situ* spectroscopic information. The *in situ* characterization reported for this reaction class is usually based on diffuse reflectance infrared Fourier transform spectroscopy (DRIFTS). Surprisingly, only four studies had the co-occurrence of the terms "*operando*" and "Eley-Rideal", indicating a dearth of pertinent spectroscopic information under/during reaction conditions, which is invaluable for discerning the surface reaction mechanisms.

Summarily, a vast majority of the analyzed studies that invoke the E-R mechanism across the four main reactions primarily rely on data fitting of experimental rate data to L-H and E-R/L-R rate equations and test for goodness of fit in the absence of spectroscopic evidence. In the next section, we present a brief discussion on the caveats of assigning reaction mechanisms based on fitting of experimental rate data in the absence of relevant experiments relying on pertinent transient, *in situ*, and *operando* spectroscopic characterization to corroborate the reaction mechanism. In our subsequent discussion, we focus on the four reactions identified above to drive our point.

2. UNDERSTANDING CAVEATS IN FITTING OF EXPERIMENTAL RATE DATA

Prior to the availability of modern catalysis science research methods and *in situ* and *operando* characterization tools, reaction mechanisms were determined predominantly by identifying the best fits of reaction rate data to idealized mathematical expressions for the various reaction mechanisms such as L-H, E-R, L-R, MvK, etc. In this section, we discuss strengths and pitfalls of various practices within reaction kinetics that are commonly used to ascertain surface reaction mechanisms.

Assuming a bimolecular reaction between reactants A and B to form C by a solid catalyst

$$A + B \rightarrow C \tag{1}$$

If this reaction proceeds via the irreversible L-H mechanism (i.e., in which A and B both chemisorb competitively on the catalyst surface prior to reacting and form C on the surface with the re-adsorption of C not taking place), the rate of production of C can be written as[1,18]

$$\mathrm{dC}\big/\mathrm{dt} = \frac{k_3 K_A K_B P_A P_B (*_o)^2}{(1 + K_A P_A + K_B P_B)^2} \tag{2}$$

where k_3 is the forward rate constant for the step involving the reaction of chemisorbed A and B species (rate-determining step, rds), K_A and K_B are the adsorption equilibrium rate constants for A and B, respectively, P_A and P_B are the gas-phase partial pressures of reactants A and B, respectively, and $(*_o)$ is the density of surface sites (total sites per unit surface area).[19,20] Therefore, the rate of a surface-catalyzed reaction will depend on a few critical factors: the gas-phase partial pressures of reactants (P_A and P_B), relative adsorption−desorption equilibrium between reactants A and B (K_A and K_B), surface site density ($*_o$), and rate constant of the rds (k_3).

The term $(*_o)^2$ results for L-H kinetics for mobile surface intermediates or surface sites. In contrast, if surface sites and adsorbates are assumed to be immobile, the square dependence is reduced to a linear dependence, i.e., $(*_o)^1$, with an added caveat that reactants adsorb on adjacent/pair sites.[21,22] In the past, the L-H derivation for immobile adsorbed intermediates on immobile pair sites was adopted, but it is now known that the surface intermediates and surface sites (especially in supported metal oxide catalysts) may both be mobile under reactions

conditions,[22,23] which corresponds to the first case; hence, we include the $(*_o)^2$ term. Additional details of L-H kinetics by mobile surface intermediates and sites can be found in our dedicated analysis.[22] It suffices to note that the rate of production of C may exhibit a second-order dependence on the surface site density $(*_o)$ if the rds is bimolecular or if two surface sites are involved in subsequent, unimolecular slow steps.[22] Examples of reactions that exhibit second-order dependence on $(*_o)$ include selective catalytic reduction of NO_x with NH_3, butane oxidation to maleic anhydride, and propene oxidation to acrolein.[22] Likewise, the rate of production of C may exhibit first-order dependence on $(*_o)$ if the rds is unimolecular even in reactions that have bimolecular stoichiometry that involve lattice oxygen from oxide catalysts (e.g., methanol oxidation with oxygen, oxidative dehydrogenation of ethane or propane, SO_2 oxidation with oxygen, etc.).[22] We direct the reader to a dedicated article on the nuances of understanding reaction orders on the surface site density for supported metal oxide catalysts.[22]

Next, if this reaction proceeds via an irreversible E-R or L-R mechanism (i.e., A is chemisorbed on the catalyst surface while B is weakly physisorbed (i.e., $K_B \ll K_A$) or in the gas phase (i.e., $K_B = 0$) to form the product C), the rate of production of C can be written as[1]

$$\frac{dC}{dt} = \frac{k_3 K_A P_A P_B (*_o)^1}{1 + K_A P_A} \tag{3}$$

In this case, the rate of production of C will exhibit a first-order dependence on the partial pressures of A and B. Importantly, the reaction rate will exhibit a first-order dependence on $(*_o)$, and the possibility of any higher orders does not exist because the probability of three body collisions of atoms/molecules is extremely low. Therefore, it is apparent that carefully collected kinetic data can be analyzed for the dependence on surface site density $(*_o)$, where the slope of the ln−ln plot of the rate vs $(*_o)$ will be ∼1 for a bimolecular reaction proceeding via E-R/L-R mechanisms and 2 for a bimolecular reaction proceeding via the L-H mechanism. If the global stoichiometry is bimolecular but the rds is unimolecular in the L-H mechanism, only then will the L-H mechanism also exhibit a slope of ∼1.

In catalysis studies, the observed reaction rate is recorded as a function of the partial pressures of the reactants (one at a time) or sometimes by varying the number of active sites or surface site density of the catalyst. The observed rate is then used to tune the rate constants to fit mathematical expressions that represent L-H vs E-R/L-R to the experimentally collected data. It is often seen that both reaction mechanisms fit the experimental data sufficiently, where the commonly reported goodness of fit parameter (R^2) is above 0.9 for both cases (see discussion within the cited references).[24,5] The reaction mechanism is then chosen based on the fit that gives the higher R^2.

As noted above, to fit the experimentally observed reaction rate data, rate constants (e.g., k_3, K_A, and K_B in the equations above) need to be tuned to maximize the goodness of fit to one of the rate expressions, which are then reported in papers. The point to highlight here is that rate constants are optimizable parameters to increase the goodness of fit for L-H and E-R/L-R models to the experimental rate data as a function of the partial pressure of the reactants, where the greater the number of such tunable parameters or rate constants involved in the expression, the better the general fit is going to be. Specifically, the expression for the L-H mechanism is dependent on both

equilibrium rate constants K_A and K_B, while the expression for the E-R or L-R mechanism is only dependent on K_A, as only one reactant adsorbs. Therefore, the L-H expression usually exhibits a better fit of the experimental data set than E-R/L-R, even when a reaction may follow an E-R/L-R mechanism. The inherent fitting bias for the L-H mechanism due to the greater number of tunable parameters has been recognized in the field,[25] and we caution practitioners to be wary of minor differences in the R^2 parameter when fitting kinetic data to L-H vs E-R/L-R models to ascertain the operable mechanism.

Assuming Langmuir's adsorption model that the surface is uniform, no lateral interactions occur, and there is one adsorbed reactant per surface catalytic site, if kinetic experiments are conducted carefully to yield high fidelity data sets under conditions that preclude mass and heat transport limitations, they can help differentiate between various mechanisms given that the parametric errors are rigorously quantified and determined to be small in comparison to the parametric magnitudes. For example, under differential conditions, the partial pressure of one reactant can be varied by 2−3 orders of magnitude (e.g., 0.5−50 kPa) while the partial pressure of the other reactant and the total pressure of the system is kept constant to understand individual equilibrium behaviors for A and B, assuming K_A and K_B differ significantly. However, we note that the assumption of "no lateral interactions" is usually incorrect in real-world systems and conditions. Studies evince systematic changes in the activation barrier of the L-H mechanism's rate-determining step with changes in reactant coverage, suggesting lateral interactions.[26]

Likewise, if K_A and K_B differ significantly (i.e., surface coverages differ significantly), partial pressure sweep experiments with respect to the stronger binding reactant will yield a negative reaction order as its partial pressure increases and the adsorption of the second (weaker binding) reactant becomes rate-limiting. Therefore, a key trend that may differentiate E-R/L-R vs L-H mechanisms is the presence of negative orders, which can indicate the prevalence of the L-H mechanism (i.e., both reactants adsorb albeit with different equilibrium constants). If the reaction follows the E-R/L-R mechanism, such a partial pressure sweep of reactants will not yield a negative order, as the reaction only depends on the adsorption of one reactant and does not depend on the adsorption of the other reactant. However, it must be ensured that during such sweeps, spectator species do not form that block the active sites to yield negative orders artificially or coverage-dependent lateral interactions do not cause repulsion and hence a negative order. Summarily, careful kinetic experiments conducted under conditions that preclude heat and mass transport limitations can yield insights to differentiate between the possible underpinning mechanisms and corroborate the surface reaction mechanism without relying on a data fitting approach solely.

Notably, as early as the 1940s, Eley recognized and cautioned against solely relying on fitting kinetic data to differentiate between catalytic reaction mechanisms on solid surfaces.[11] In this regard, we present a brief exercise in reaction rate analysis in the L-H vs E-R/L-R mechanisms to highlight strengths and limitations of such a mathematical fitting approach using reasonable artificial data. The effect of parameter variation on the reaction rates was investigated as follows: P_A and P_B were kept constant at 0.5 each, while rate constants K_A and K_B were varied by orders of magnitude along with the surface density of catalytic sites $(*_o)$, as shown in Figure 2. The resulting reaction

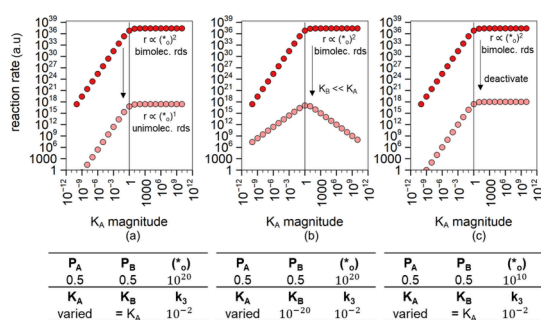rates are compared between the L-H vs E-R/L-R mechanisms in Figure 2.

Figure 2. Understanding L-H reaction rate as a function of (a) simultaneously changing K_A and K_B, where $K_A = K_B$, assuming a bimolecular vs unimolecular rds; (b) varying K_A while K_B is held constant such that $K_B \ll K_A$ for a bimolecular reaction, while the surface site density is unchanged; and (c) simultaneously changing K_A and K_B, where $K_A = K_B$ but the surface site density is reduced. The vertical line at $K_A = 1$ is presented to draw the eye toward regions qualitatively representing strong binding of reactant A. For simplicity and clarity, we refrain from specifying exact units of rate and rate constants and instead use arbitrary units (a.u.), as the actual units would depend on the units of partial pressures, catalyst mass, and site density used in the kinetic expression.

The rate of reaction was first calculated for a reaction represented by eq 1, where K_A and K_B were varied simultaneously such that K_A and K_B were equal (arbitrary units, a.u.), while k_3 was held constant at 10^{-2} (a.u.) and $(*_o) = 10^{20}$ sites/unit area (Figure 2a). The pink data points represent an L-H reaction occurring via a unimolecular rds such that rate $\propto (*_o)^1$, in contrast to one occurring via a bimolecular rds where rate $\propto (*_o)^2$. Next, the reaction rate was calculated by varying K_A, while K_B was held constant at an extremely low value (10^{-20}) to signify a case where one reactant preferentially adsorbs on the catalyst surface and maintains a high coverage, with k_3 and $(*_o)$ still equal to 10^{-2} and 10^{20}, respectively (Figure 2b). In comparison to the reference rate curve where $K_A = K_B$, the rate curve generated by assuming $K_A \gg K_B$ exhibits a volcano-type shape, where the rate increases as K_A increases until a value of 1, beyond which the rate decreases as the surface becomes deficient in B species that also need to adsorb for the bimolecular reaction to occur. Finally, we depict the effect of reducing the surface site density to signify poisoning and deactivation in Figure 2c. The reaction rate curve maintains its shape as in the reference case but simply shifts downward to lower values. These scenarios demonstrate various limiting cases that need to be kept in mind when analyzing experimental rate data in the framework of the idealized L-H expression, as the rate will be impacted by orders of magnitude due to the underlying reaction dynamics and mechanism.

The reaction in eq 1 is next compared in terms of the L-H ratio (eq 2) vs E-R/L-R (eq 3) mechanisms. The rates of reaction are compared as K_A is varied in the same range for L-H and E-R/L-R scenarios, while all other parameters are kept constant between the two scenarios (i.e., $P_A = P_B = 0.5$, $k_3 = 1.0^{-2}$, $(*_o) = 10^{20}$), as shown in Figure 3a. Under these assumptions, the rate of reaction in the case of a bimolecular reaction occurring via the E-R/L-R mechanism is lower than the L-H mechanism, assuming that the rds in L-H is also bimolecular—a difference that can help distinguish between the two mechanisms in this idealized
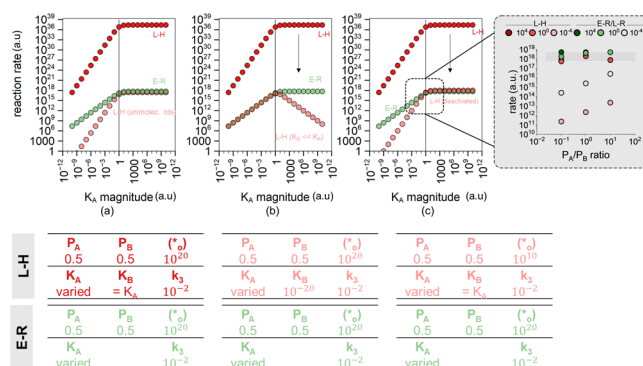

Figure 3. Comparing the rate of reaction as a function of (left) L-H vs E-R/L-R pathways such that all parameters are equivalent between the two pathways; (center) L-H vs E-R/L-R pathways such that A adsorbs preferentially over B during the L-H mechanism; and (right) L-H vs E-R/L-R such that in the case of the L-H mechanism, most of the sites are poisoned/deactivated. The inset in the right plot shows the reaction rate as the partial pressure of A is swept 3 orders of magnitude (0.5 to 5 to 50) while the partial pressure of B is kept constant (at 5), leading to a change in P_A/P_B from 0.1 to 10. It is seen that as equilibrium constants are varied 10^{-4} to 10^0 to 10^4 ($K_A = K_B$), the resulting reaction rates are practically indistinguishable (within 1 order of magnitude; dark gray region) between L-H and E-R/L-R for $K_A > 1$ for high surface coverage of reactant(s).

case. The underlying reason for the higher rate via L-H is the quadratic dependence of the rate on $(*_o)$. If a unimolecular rds is assumed for the L-H case instead, the reaction rate then becomes identical to the E-R case as the quadratic dependence changes to a linear dependence on $(*_o)$. This analysis shows that if the surface reaction is strictly bimolecular and every parameter is held identical between the L-H and E-R/L-R cases, the reaction rate would be higher for the L-H case owing to the nonlinear dependence—an observation that can help differentiate the two in practical catalysis. However, the L-H (bimolecular rds) reaction rates become identical or at least indistinguishable from a practical standpoint with the rates in the E-R/L-R mechanism in a certain range of K_A magnitude if the two limiting conditions are applied to the L-H scenario: (i) if K_B is miniscule in comparison to K_A, i.e., the surface coverage of B is extremely low (Figure 3b), and (ii) if most of the sites are poisoned, specifically those that bind reactant B (Figure 3c).

This exercise is summarized in Figure 3, which highlights that although fitting experimental rate data to L-H and E-R/L-R models can help distinguish between the various reaction mechanisms in idealized cases where reaction rates and reaction dynamics are expected to differ significantly between various surface reaction mechanisms, under realistic experimental conditions, the various mechanisms cannot always be reliably distinguished using rate analyses. Furthermore, depending on the K_A and K_B magnitudes, the experimental rate data might fit both L-H and E-R/L-R models well enough, making it exceeding challenging to use R^2 values to differentiate between operable mechanism. In practical catalysis, catalysts are experiencing deactivation, sintering, poisoning, and restructuring as a function of time on stream that further complicate the situation.[16] Moreover, competitive/preferential adsorption between two reactant species usually occurs, and product re-adsorption is also typically a concern.[16] Such complications can create scenarios where the apparent rate of a reaction proceeding via the L-H mechanism would appear indistinguishable from the reaction proceeding via the E-R/L-R mechanism, as highlighted

in Figure 3, unless an impractically wide range of partial pressures is investigated to find a region where rates become distinguishable, akin to the impractically wide range of K values studied in Figure 3. We further highlight this point in the inset of Figure 3c, where even when sweeping the partial pressure of A 3 orders of magnitude while keeping the partial pressure of B constant, the reaction rates are indistinguishable in L-H vs E-R/L-R mechanisms when $K_A > 1$ (A adsorbs strongly). In summary, practitioners are discouraged to solely rely on data fitting to ascertain reaction mechanisms since similar equilibrium constants coupled with nonidealities in the system can yield sufficiently high goodness of fit for all mechanisms. When rate analyses are used, practitioners are advised to measure adsorption equilibrium constants independently via chemisorption experiments and compare them to the values for such constants provided by data fitting to assess whether these fitted parameters are realistic. Alternatively, if adsorption equilibrium constants are measured independently, they could be treated as fixed "constants" in the model fitting algorithm, and this can reduce the number of floating variables in the model that is regressed to the data. However, a caveat to remember is that these equilibrium constants should only constitute adsorption–desorption and not reaction steps, which is sometimes impossible to separate at reaction relevant conditions.

Important caveats to be considered for using kinetic arguments to differentiate between L-H vs E-R/L-R mechanisms include:

i. If both reactants A and B are weakly adsorbing (i.e., surface coverages of both A and B are low and most of the sites remain vacant), it becomes practically impossible to use kinetic data to ascertain L-H vs E-R, as the rate of reaction will not vary significantly with changes in the surface density of sites.[27]

ii. If the reactant(s) adsorb strongly on surface sites (i.e., surface coverages are high), in the case of L-H, the reaction rate will be proportional to the square of the number of sites if the rds is bimolecular or if two unimolecular rds occur on two different sites (i.e., r $\propto$ $(*_o)^2$).[22,28,29] If the rds is unimolecular, as is often noted in simple two-electron oxidations like CH_3OH oxidation, oxidative dehydrogenation of alkanes, etc., the rate will vary linearly with $(*_o)$ (i.e., r $\propto$ $(*_o)^1$).[22,28] Conversely, if the E-R/L-R mechanism is operable, the rate will be linearly proportional to the number of catalytic sites, as only one reactant chemisorbs (i.e., rate $\propto$ $(*_o)^1$).

iii. In rare cases, A and B can co-adsorb on the same catalytic site instead of two adjacent sites even when the L-H-type mechanism is followed. For example, in alkene dimerization or polymerization over heterogeneous catalysts via the so-called Cossee–Arlman mechanism, both alkene species chemisorb on the same catalytic center sequentially to form the product.[30−32] In such a scenario, the rate will vary linearly with the surface density of sites, and square dependence will not be observed even when the E-R/L-R-type mechanism is not operating. Hence, in such cases, distinguishing E-R/L-R vs L-H using rate vs surface site density analysis is not possible.

Noting the above caveats, carefully synthesized and thoroughly characterized catalysts may be used to study the rate dependence on the catalytic site population, where an example of this methodology was reported in a study of NH_3 selective catalytic reduction of NO_x over supported V_2O_5-WO_3/

TiO_2 catalysts.[29] For this catalytic reaction, the reaction rate exhibited a second-order dependence with respect to the variation in the number of catalytic sites (i.e., the rate quadrupled when the number of sites doubled). This behavior confirmed that a two-site L-H mechanism was at play with both surface NH_3 and NO adsorbed on the catalyst, in contrast to the often-invoked single-site E-R/L-R mechanism for this catalytic reaction.[29] This conclusion is corroborated by a modulation-excitation spectroscopy study, which provides direct spectroscopic evidence of the NH_2NO^* surface intermediate being present,[33] confirming that indeed both NO and NH_3 reactants adsorbed on the catalyst surface during SCR, as expected for the L-H mechanism.

At this point, a few considerations regarding the active sites themselves also need to be discussed. We note that the concept of active sites is not the same under all schools of thought: the Langmuir school of thought argues that all exposed sites are equal and active (often called mean-field approximation associated with uniform surface sites), while the Taylor school of thought argues that only a fraction of the total exposed sites constitute the true active sites.[34,35] Counting the number of active sites accurately, therefore, is not a trivial task and depends on which school of thought is followed since the number of sites can vary by orders of magnitude in a catalytic material depending on the definition. While practitioners are free to choose either viewpoint, they should adhere to the chosen definition of the active sites and the site counting method across their studies and catalysts to make comparison fair and to extract meaningful kinetic and mechanistic data. Furthermore, while the number of active sites can be varied via controlled synthesis of the catalyst (for example, by changing the mass loading of the active metal or surface metal oxide coverage in supported metal oxide catalysts), synthesis should be coupled with spectroscopic analysis and chemical probes to ensure that the nature of those sites is well-defined and arguably similar (i.e., all sites are dispersed, all sites have similar nuclearity across the samples, etc.). If changing the population of sites inadvertently leads to a change in the nature (molecular and electronic structure) of those active sites, correlating the reaction rate with the number of active sites to differentiate between L-H vs E-R/L-R mechanisms may become problematic and potentially misleading. Taken together, information regarding generalized measures of activity and the active sites needs to be carefully collected under conditions that preclude transport limitations and actually involve a change in the concentration of the active sites.[35]

3. EXPERIMENTAL AND COMPUTATIONAL METHODS TO RELIABLY DISTINGUISH BETWEEN L-H VS E-R/L-R MECHANISMS

In the previous sections, we highlighted limitations of kinetic/rate data analysis to differentiate between various surface mechanisms, which leads to the following question: what other tools and/or techniques can be used to differentiate the likely surface mechanism more reliably? In this section, we provide our perspective on promising techniques/tools that can augment efforts toward differentiating between E-R/L-R and L-H mechanisms in heterogeneous catalysis and provide insights to discern the operable surface reaction mechanism. The underlying factor that makes these experimental techniques unique is that they do not rely on indirect inferences and data fitting and instead rely on the direct observations and responses of either the surface or the gas-phase species as a function of reaction conditions.
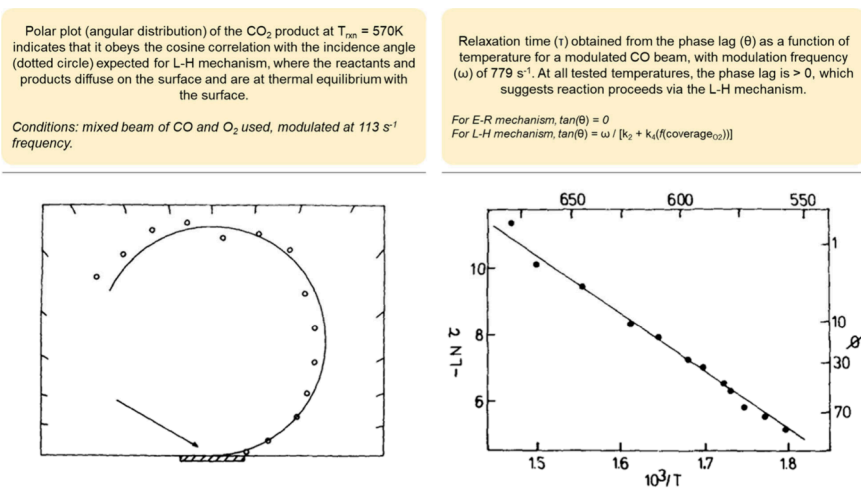
Figure 4. Summarized results suggesting that the catalytic formation of CO_2 on Pd (111) proceeds via the L-H mechanism and not the E-R mechanism as often speculated. Left panel represents a polar plot of the angular distribution of the CO_2 formed, which follows a cosine distribution expected for the L-H mechanism. Right panel summarizes results of the phase lag (θ) as a function of reaction temperature. Reproduced with permission from ref 38. Copyright 1978, AIP Publishing.

3.1. Molecular Beam Spectroscopy (MBS).

Molecular beams (steady and modulated/chopped) where the energy and direction of the molecules constituting the beam are carefully controlled have been used in kinetic studies on ideal surfaces (single crystals) to introduce gas-phase reacting species into the ultrahigh vacuum (UHV) environment typically used in such research to maintain surface cleanliness.[36] The beam is directed at the solid surface of interest, where surface reactions (typically single collision events) may lead to the formation of new products. The scattered reactants and products are then detected, identified, and quantified usually by using a mass spectrometer in a spatially and temporally resolved manner, which can provide direct insights regarding the operating surface mechanism, as signified by the examples discussed in the following paragraphs.[36] Experimental proof for a reaction occurring via the E-R/L-R mechanism can be gleaned by probing how much "memory effect" is observed in the products coming from the catalyst surface. The idea is that in the E-R/L-H mechanism, the reactant molecules spend a very short duration on the catalyst surface (tens of collisions depending on the catalytic metal being studied),[37] do not come to thermal equilibrium with the catalyst surface, and hence maintain significant "memory" of the gas phase. This memory effect is usually probed in two ways to check for the presence of the E-R/L-R mechanism by varying the incidence angle, the velocity of the reactant molecular beam, and the catalyst's temperature and measuring how the reaction rate, the angular distribution, and the temperature of the product desorbing from the surface vary with those parameters. If the reaction occurs via the E-R/L-R mechanism, the reaction rate will vary differently than expected based on sticking probabilities, and the desorbing product's angular distribution and velocity will be aligned with the incident beam.

We note that molecular beam spectroscopy is the only technique that may be able to distinguish between E-R and L-R mechanisms, as defined by the original authors. Specifically, the reactant being gas-phase vs physisorbed vs chemisorbed may be distinguishable based on the surface residence time as follows:

i. If the residence time of the reactant species is long enough that they thermalize with the surface (i.e., equilibrate its degrees of freedom to the surface temperature), it will lose all "memory" of its gas-phase trajectory, constituting a reaction between chemisorbed species, as in the L-H mechanism.

ii. If the residence time is on the order of magnitude of the vibrational period (10^{-13} s), the reactant will retain nearly all memory of its gas-phase trajectory, constituting a reaction occurring via species from the gas-phase colliding with the catalyst surface, as in the L-R mechanism.

iii. If the residence time is short enough that the reactive species do not thermalize, but it is order(s) of magnitude higher than the vibrational period (10^{-13} s), say, 10^{-3}–10^{-6} s, the reactant will retain some memory of its gas-phase trajectory but less so than when the residence time is ~10^{-13} s, constituting a reaction between physisorbed and chemisorbed species, as in the E-R mechanism.

Ertl's seminal works from the 1970s to the 1980s on elucidating the mechanism of CO oxidation over several single-crystal metal catalysts (Pd (111),[38] Pt (111), etc.) by application of modulated molecular beam studies provided some of the most direct pieces of evidence corroborating the prevalence of the L-H mechanism during CO oxidation under all conditions in contrast to the long-postulated E-R mechanism for this reaction.[38] Ertl's molecular beam studies also elegantly showed that the time lag observed for CO_2 production upon shooting a molecular beam of CO onto an oxygen saturated catalyst surface was far greater than the time lag expected for the E-R mechanism, where CO would not chemisorb before the reaction, and hence, CO_2 would very quickly evolve (quicker than the time resolution of the instrument of ~10 μs).[39] Likewise, phase-sensitive detection during modulated nonstationary molecular beam studies where an oxygen molecular beam is modulated while the CO pressure is held constant evinced that L-H prevailed, as the trends in phase lag between the CO_2 evolved and the molecular O_2 beam modulation were not compatible with the E-R mechanism (Figure 4). Moreover, the angular distribution of CO_2 evolved during the molecular beam studies on Pd (111) and Pt (111) was found to closely follow the cosine distribution expected for an L-H product that diffuses on the surface and is in thermal equilibrium with the surface (Figure 4).
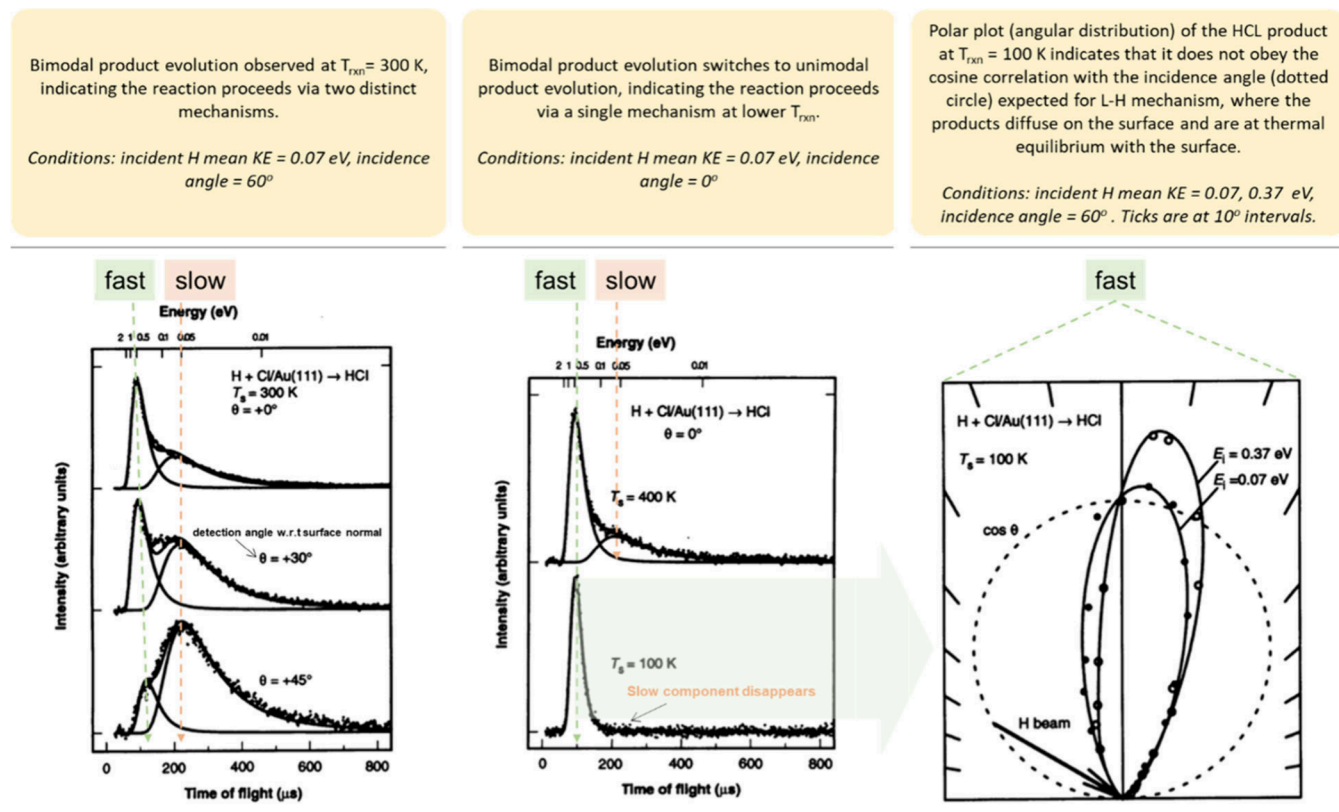
Bimodal product evolution observed at T_{rxn} = 300 K, indicating the reaction proceeds via two distinct mechanisms.

Conditions: incident H mean KE = 0.07 eV, incidence angle = 60°

Bimodal product evolution switches to unimodal product evolution, indicating the reaction proceeds via a single mechanism at lower T_{rxn}.

Conditions: incident H mean KE = 0.07 eV, incidence angle = 0°

Polar plot (angular distribution) of the HCL product at T_{rxn} = 100 K indicates that it does not obey the cosine correlation with the incidence angle (dotted circle) expected for L-H mechanism, where the products diffuse on the surface and are at thermal equilibrium with the surface.

Conditions: incident H mean KE = 0.07, 0.37 eV, incidence angle = 60°. Ticks are at 10° intervals.

Figure 5. Summarized results suggesting that the catalytic formation of HCl on Au (111) proceeds via two distinct reaction mechanisms, where E-R/L-R results in the fast product evolution and L-H results in the slow product evolution. Left and center panels represent time-of-flight measurements, while the right panel represents a polar plot of the angular distribution of the HCl formed. Reproduced with permission from ref 42. Copyright 1994, AAAS.

Importantly, Ertl's work signified that often in practical scenarios, as was observed in the case of CO oxidation, the rates of reaction may not be expressed as the product of a bimolecular rate constant and the surface coverage of the two adsorbed species, as would be expected for a simple bimolecular L-H mechanism. Instead, Ertl showed that underlying assumptions used to derive the L-H mechanism often break down under realistic catalytic reactions where competitive adsorption occurs between the two reactants, which further serves as a strong deterrent against fitting data and blindly concluding mechanisms based on just kinetic fits.[39] Ertl's molecular beam studies on CO adsorption and reaction,[40,13] in conjunction with his other molecular beam studies on NO adsorption and oxidation,[41] have thoroughly shown the complexity of adsorption in simple reactions that can lead to nonideal reaction kinetics that cannot be quantitatively described by idealized L-H and E-R/L-R rate expressions.

Ertl's proof that CO oxidation proceeds via the L-H mechanism on Pt and Pd, in conjunction with transient flash desorption studies from Campbell et al. on other transition metals like Rh also evincing CO oxidation occurring via the L-H mechanism,[37] however, should not be interpreted to mean that E-R and L-R mechanisms do not exist. For example, evidence for the E-R/L-R mechanism operating in conjunction with the L-H mechanism also came from molecular beam studies on the catalytic reaction of H atoms with chemisorbed Cl atoms to produce HCl on a metallic Au (111) catalyst.[42] Select results from this study indicating the co-occurrence of E-R and L-H mechanisms are adapted and summarized in Figure 5.

Researchers at IBM found that as the H atom beam impinged on the catalyst surface, product evolution was bimodal with a fast and slow component. They argued that bimodal product evolution indicated that two distinct reaction mechanisms were at play. The fast component was attributed to the E-R mechanism, where the product (HCl) desorbed from the surface almost instantaneously with a high kinetic energy in a narrow angular distribution that correlated to the angle and mean kinetic energy of the incident atomic H beam—called the "memory effect" in molecular beam spectroscopy literature. This fast component is understood to originate from the desorption of molecules that did not spend enough time on the surface to thermally equilibrate with the catalyst.[42] On the other hand, the slow component was understood to be coming from the L-H mechanism, where the reaction product is in thermal equilibrium with the catalyst surface, and an angular distribution of the desorbing product was close to that of a cosine function, in agreement with Ertl's work showing a similar cosine dependence when the L-H mechanism prevails. It should be noted here that the original authors of this study do not distinguish between the actual E-R and L-R mechanisms, and thus, their use of the E-R terminology should be interpreted to encompass both the E-R and L-R mechanisms.[42]

In summary, molecular beam spectroscopy can provide unparalleled and quantitative insights into the surface reaction mechanism by allowing for the direct detection of reaction products scattering off a solid catalyst surface in a spatially and temporally resolved manner. Molecular beam spectroscopy insights are especially powerful to also deconvolute parallel
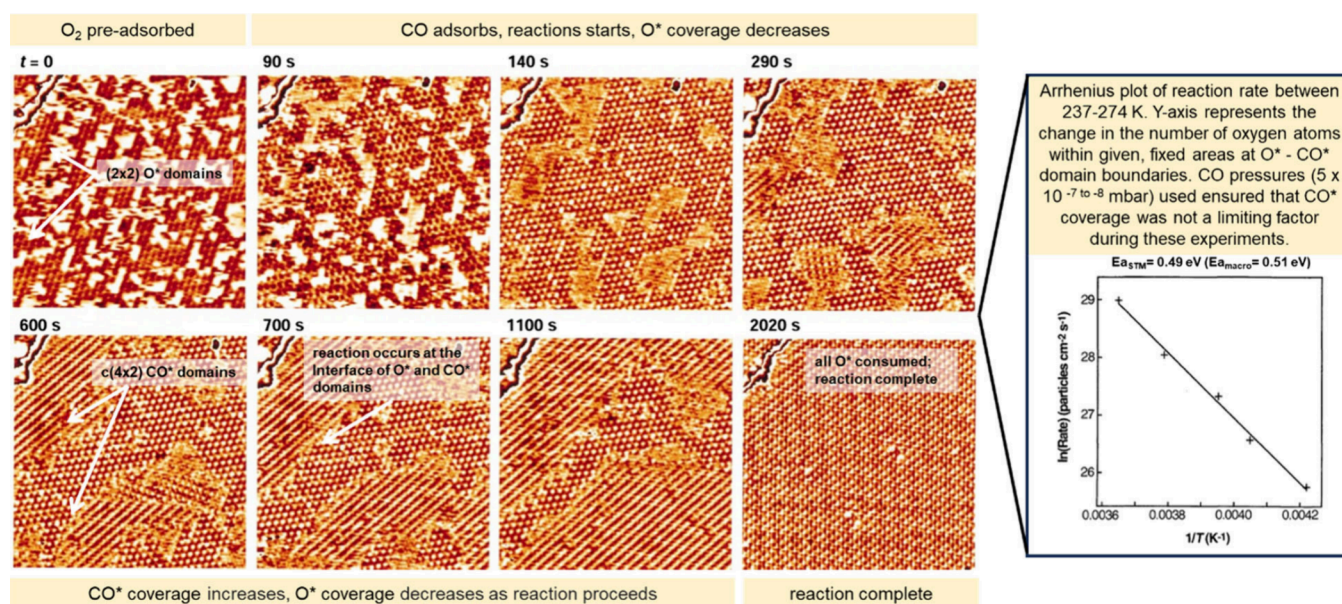
Figure 6. Series of STM images, recorded during the reaction of preadsorbed oxygen atoms with CO molecules at 247 K, all from the same area of a Pt (111) crystal. The times refer to the start of the CO exposure. The structure in the upper left corner is an atomic step of the Pt surface. Image sizes are 180 × 170 Å. Tunneling voltage (with respect to the sample), 0.5 V; tunneling current, 0.8 nA. These STM results clearly show distinct domains of adsorbed O* and CO* and the reaction occurring at the atomic interface of the two domains. The activation energy calculated from the atomic interface (rate of O* decreases at domain boundaries) was estimated to be 0.49 eV, which is in excellent agreement with the activation energy of this reaction on this catalyst estimated from the macroscale rate of reaction. Reproduced with permission from ref 54. Copyright 1997, AAAS.

pathways if more than one surface mechanism might simultaneously be at play.

3.1.1. Limitations. Molecular beam spectroscopy has historically been used by the surface science community, especially prior to the modern catalysis science and engineering era, to study simple reactions on model, atomically flat single-crystal metal catalysts, and epitaxial thin metal oxide films.[43] Commonly studied reactions include H activation like H_2-D_2 isotope-scrambling, CO oxidation, H_2 oxidation, NO oxidation, HCOOH decomposition, etc.[44,45] The application of molecular beam spectroscopy for more complex systems is lacking, due to the complexity and capital investment required for the molecular beam setup for more complicated reactions.[36] Moreover, the stringent requirement that precludes the widespread application of this informative technique is the atomically flat single-crystal nature of the solid catalyst required to scatter the molecular beam from the surface. In contrast, commonly used powdered catalysts such as supported metals or metal oxides, however, have rough surfaces and are not compatible with studying with molecular beam spectroscopy.

3.2. Scanning Tunneling Microscopy/Spectroscopy (STM/STS). The fundamental principle of STM is as follows: an atomically sharp metal tip is brought into close proximity (3–5 Å) of a conductive surface, allowing an overlap between the tip and the electronic wave functions of the conductive surface.[46] A bias voltage applied between the tip and the surface allows electrons to tunnel through the vacuum (junction gap), separating them. The resulting tunneling current is a function of the tip position, applied voltage, and local density of states (LDOS) of the sample.[46] STM can provide deep insights into the structure of the surface being analyzed, even for complex surfaces that are not fully ordered or are undergoing dynamic restructuring.[47] STM images of a conductive surface can be used to calculate average ensemble sizes with a spatial accuracy of 0.1 nm and a depth resolution of 0.01 nm to relate ensemble size

with observed properties like catalytic activity.[48,49] Finally, STM can be used to resolve the structure of bare surfaces before, after, and during reaction with atomic resolution, making STM a powerful technique for fundamental catalysis science research. STM images are usually interpreted in the framework of the Tersoff–Hamann model,[48–50] in which an STM image represents a contour map of constant LDOS of the sample at the Fermi energy (E_F), analyzed at the position of the tip.[48,49]

Likewise, scanning tunneling spectroscopy (STS) works by placing a scanning tunneling microscope tip above a particular spot on a conductive sample. With the height of the tip fixed, the electron tunneling current is then measured as a function of electron energy by varying the voltage between the tip and the sample. The change of the current with the energy of the electrons is the simplest spectrum that can be obtained.[48,49] Plots of the normalized conductance $(dI/dV)/(I/V)$ vs V provide spectra of the electronic state density (occupied and empty) at these locations with atomic resolution.[48,49]

Unlike most surface science tools that require ultrahigh vacuum (UHV), STM is not limited to operate under the extremely idealized UHV conditions, and it is thus possible to perform *in situ* STM studies at high pressures and temperatures (up to 1–5 bar and up to 600 K),[51,52] whereby the reaction conditions for most practical catalysis are approached.[46] Since the first report on atomically resolved STM images of the Au (111) surface in 1987,[53] STM has matured tremendously to become a robust analytical tool that provides atomically resolved insights on atomic and molecular dynamics, adsorbate-induced restructuring on surfaces, and chemical reactions on surfaces with relevance to heterogeneous catalysis.[46] STM/STS is especially beneficial to provide useful atomic and molecular level insights regarding the underlying surface reaction mechanism, as catalytic surfaces can be imaged and characterized directly under reaction conditions to identify and quantify the adsorbates on the surface.
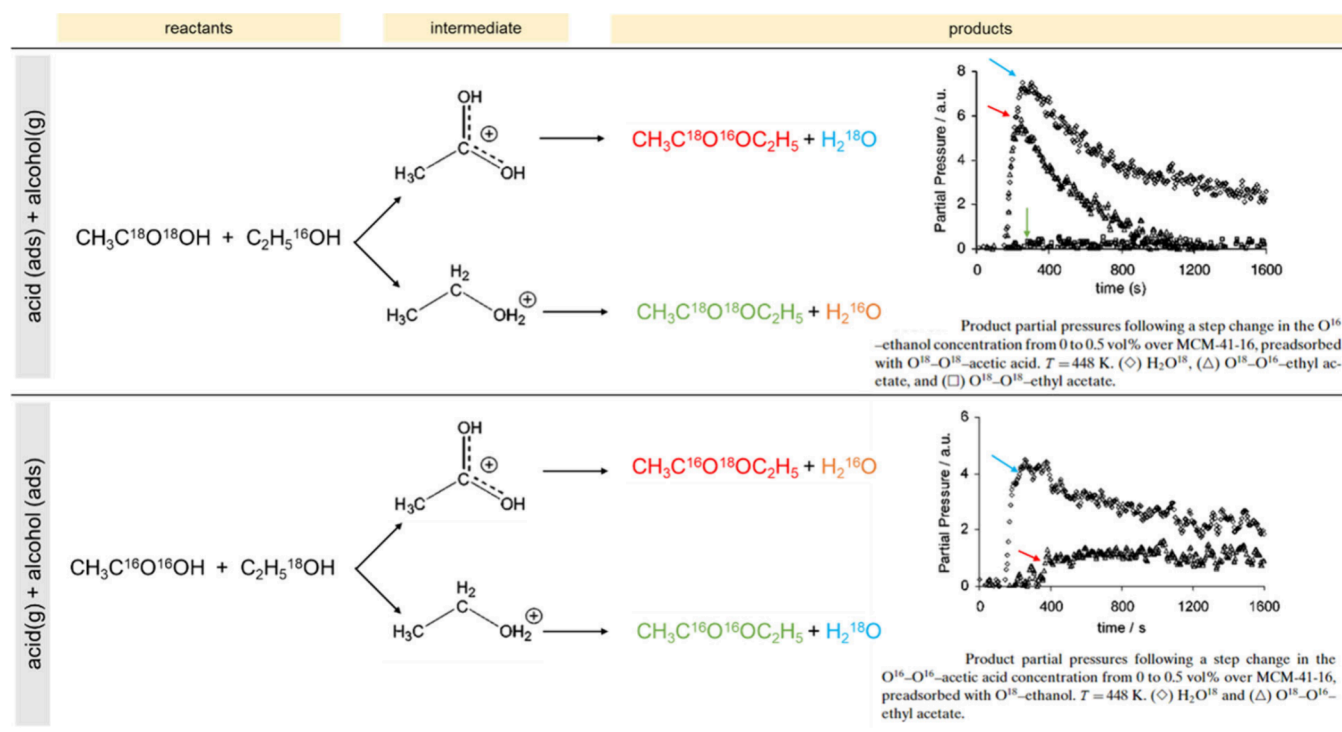
Figure 7. Summarized results of isotope-switch experiments at 448 K, evincing that esterification of acetic acid and ethanol proceeds via the L-H mechanism with both reactants adsorbed on the solid acid catalyst (MCM-41 SAR 16) used in the study. The reaction was shown to proceed via a protonated acetic acid intermediate, which yields mixed-isotope ester product (red) in both configurations tested: (top) acid (ads) + alcohol (g); (bottom) acid (g) + alcohol (ads). The production of $H_2^{18}O$ in the bottom panel is unexpected, as $H_2^{16}O$ should have evolved noting the protonated acetic acid intermediate. However, control experiments in temperature-programmed mode (not shown here) in the original study suggest that the $H_2^{18}O$ is a product of labeled ethanol dehydration during adsorption with the coevolution of diethyl ether. The $^{16}O-^{16}O$ ester product (green) in the bottom panel does not form. Reproduced with permission from ref 56. Copyright 2001, Elsevier.

For example, a pioneering and one of the most elegant uses of STM toward catalysis was reported by Ertl et al. in the 1990s, where *in situ* STM was used to study CO oxidation on Pt (111).[54] In this work, as summarized in Figure 6, the microscopic reaction rate was quantified from the sequence of STM images and found to be proportional to the edge length along the phase boundary of surface CO* and O* domains or islands on the catalyst surface rather than to the product of the reactants surface coverage, as one would have expected from a simple L-H model.[54] The findings from this STM study are in good agreement with Ertl's aforementioned molecular beam studies showing the inadequacy of the idealized L-H model and directly show that both CO and O₂ reactants are indeed adsorbed on the catalyst surface prior to reaction—an observation not compatible with the E-R/L-R mechanism often incorrectly invoked to describe catalytic CO oxidation on PGM catalysts.

In summary, STM/STS can be used to study surface adsorbed species in a temporally and spatially resolved manner, which can in turn provide direct and quantitative evidence to confirm the surface reaction mechanism as well as provide an alternate route (instead of using steady-state flow reactors) for the estimation of reaction rates and activation barriers.

3.2.1. Limitations. The tunneling contact can possibly be problematic for STM studies of conductive solid catalysts, as the surface processes may be affected by the STM tip.[49] The forces from the orbital overlap between the instrument tip and the surface are expected to also influence the adsorbates by the tunneling current (leading to excitations of the adsorbate complexes) and by the electric field between the tip and the

sample.[49] Lastly, the tip could also perturb the flow of particles to and from the gas phase by geometric shielding of the space above the area under investigation, creating artifacts in the observed results, unless parameters are carefully chosen. We also direct the reader to an excellent review[55] that highlights how certain nuances in STM/STS data can mislead the researcher if they are not cross verified with other advanced techniques used for studying kinetics of elementary reactions. An important word of caution to bear in mind is that STM cannot easily differentiate/distinguish between the nature of species on the surface, e.g., if there is a dimer or monomer of a certain surface species. Moreover, STM can also not differentiate directly between active surface species and spectator species, and so the STM images need to be collected as a function of the gaseous environment and temperature to quantify the changes in the population of the surface adsorbates in the STM images. STM necessitates that the experiments are performed in conjunction with the necessary controls to ensure meaningful analysis.

3.3. Isotope-Switch and Transient Studies. Isotope-switch experiments, both in steady-state and transient modes, can yield valuable information regarding the reaction kinetics and mechanism, as isotopically labeled reactants and products are easily quantifiable by online mass spectrometers. Therefore, if an atom involved in the rds is substituted with an isotopically labeled reactant (i.e., a heavier isotope), the kinetics of the rds retard—an observation that can be used to verify the rds in a multistep reaction—and the identity of the product(s) with the heavier isotope can also confirm or rule out the underlying surface mechanism.

An example of transient experiments employing isotope-switch experiments to differentiate between L-H vs E-R/L-R mechanisms is that of gaseous ethanol and acetic acid esterification in acidic zeolite catalysts.[31] As discussed in the Introduction section, esterification reactions are one of the four classes of reactions where the E-R mechanism is extensively invoked; therefore, we highlight this example to shed some light on this class of reaction, as previous sections already discussed examples of the other three classes of reactions (i.e., CO oxidation, NH_3 SCR of NO_x, and H activation).

Esterification of gaseous acetic acid with alcohols such as ethanol over heterogeneous solid acid catalysts is a promising route to produce industrially relevant ester products while circumventing homogeneous catalytic routes that utilize concentrated liquid sulfuric acid. Various groups studying such esterification reactions have invoked both the L-H and E-R mechanisms based on the fitting of kinetic data, but a consensus was lacking until isotope-switch experiments were performed. In a seminal study, as summarized in Figure 7, experiments were conducted where an isotopically labeled O^{18}-containing reactant was preadsorbed on the MCM-41 catalyst, while an unlabeled (O^{16}-containing) gaseous reactant was then flown over the catalyst.[56] Results of isotope-switch experiments with pre-adsorbed O^{18}-labeled acetic acid and O^{16}−ethanol in the gas phase revealed the production of O^{18}-containing $H_2^{18}O$ and an O^{18}−O^{16}-containing ester. These products could only form if the reaction occurred via an L-H mechanism with a protonated acetic acid reactive intermediate populating the catalyst surface (instead of the protonated ethanol intermediate).[56] When the inverse experiment was conducted (i.e., unlabeled acid in the gas phase with ^{18}O-labeled ethanol preadsorbed on the catalyst), once again the mixed ester containing ^{18}O−^{16}O evolved (Figure 7). Production of the mixed ester confirmed that this reaction occurs via the L-H mechanism with both reactants adsorbed on the surface and surface-bound, protonated acid is the reactive surface intermediate. These results are incompatible with E-R/L-R mechanisms hypothesized in many studies for such esterification reactions, where the acid is often thought to be in the gas phase and not on the surface.

In the same study, transient experiments of unlabeled reactants such that either ethanol was preadsorbed while acetic acid was in the gas phase or acetic acid was preadsorbed and ethanol was in the gas phase further confirmed that, indeed, both reactants must adsorb before the ethyl acetate product was detected, which further ruled out the possibility of the E-R/L-R mechanism.[56] Lastly, a used catalyst sample was subjected to an oxidative temperature-programmed desorption (TPD) experiment after reaction, where the production of C_2H_4 (and H_2O from the dehydration of chemisorbed C_2H_5OH) and CO_2 (and CH_4 from the decomposition of CH_3COOH) were monitored. The TPD experiments confirmed the evolution of C_2H_4 and CO_2, which once again confirmed that both acid and alcohol reactants were chemisorbed on the catalyst surface, in agreement with the L-H mechanism.[56] In summary, carefully designed temperature-programmed and transient experiments involving isotope-switches are required to unambiguously ascertain the reaction mechanism and identify the dominant reaction pathway if multiple paths involving unique reactive surface intermediates are feasible.

In conclusion, transient experiments, especially those using isotope-switches, can provide unambiguous information to confirm the surface reaction mechanism and elucidate the reactive surface intermediates and the rds of a catalytic cycle.

3.3.1. Limitations. We note that although isotope-switch experiments will yield useful, unambiguous information that can help differentiate between L-H vs E-R/L-R mechanisms and identify reactive surface intermediates associated with each mechanism, the reactors used for isotope-switches need to be well-maintained and thoroughly characterized to account for hydrodynamic gradients, dead-volumes, valve-switching times, etc., to avoid pitfalls in data analysis and interpretation. One commonly applied approach to account for hydrodynamic gradients and reactor dead-volume is to introduce a small concentration of an inert tracer in the isotope-switch experiments in either of the isotopes, as detailed in a dedicated review on the topic.[57] Further, care must be taken when interpreting results in light of control experiments because rapid isotopic-scrambling by some sites on catalysts can lead to misinterpretations by producing mixed-isotope products that can convolute the findings. Lastly, it is worth noting that isotopically labeled reactants are typically costly and can take significantly longer to acquire commercially in comparison with their unlabeled counterparts. The price and availability of such resources can sometimes preclude researchers from performing repeat experiments when they observe unexpected results. While transient experiments have sometimes been able to provide the desired information without the use of expensive isotopes (i.e., discrimination between L-H and MvK mechanisms),[58] we note that transient studies should be designed and conducted carefully by employing clean, well-characterized, low-dead-volume differential reactors.

3.4. Computational Modeling. Density functional theory (DFT) studies are one of the cornerstones of modern catalysis science research. Traditionally, DFT has been used to compute the energy barrier for a given reaction pathway occurring on a specific catalytic site configuration, and the magnitudes of the computed barriers are then used to argue for the most feasible/likely reaction pathway. Numerous DFT studies have attempted to differentiate between the more likely reaction mechanism between L-H and E-R/L-R possibilities for various reactions, especially the four main reaction classes identified in the Introduction section.[59] For example, $CO_{(g)}$ oxidation to CO_2 with $O_{2(g)}$ over Pt (111) was studied via DFT.[60] It was found that the reaction barrier from the E-R pathway (i.e., CO does not chemisorb before the reaction) was ~0.50−0.70 eV lower than that of the L-H pathway (i.e., CO and O_2 both chemisorb before the reaction), even though this reaction was experimentally proven to be proceeding via the L-H mechanism, as discussed in earlier sections.[60] The authors of this DFT study explained that although the reaction barrier for the E-R pathway was lower, the reaction would still proceed via the L-H pathway, given the following two considerations:

i. The E-R mechanism involves a very specific configurational path where factors such as the tilting of CO and the activation of chemisorbed O atoms become critical. The average bond length of Pt−O was found to be 2.20 Å in the E-R transition state, compared to 2.02 Å in the initial state. Minor changes in the transition state (from suboptimal CO tilt, approach angle, etc.) were found to result in a large increase in the energy barrier of the E-R pathway, sometimes enough to increase the E-R barrier to a magnitude larger than the L-H barrier.[60] Note that this point raised by the original authors is in line with our point of view, presented in the Introduction, on the importance of accounting for the nuanced difference

between the L-R (gas-phase reacting with chemisorbed species) and E-R (physisorbed reacting with chemisorbed species) mechanisms. The reaction barrier is clearly very sensitive to the initial state of the nonchemisorbed species, where factors like attack angle, tilt, distance, etc., with respect to the chemisorbed species become important.

   ii. The E-R mechanism is essentially single-shot (i.e., if the CO fails to react with the chemisorbed O atoms, it will bounce off the surface and will not get a chance to react again). On the other hand, in the L-H pathway, since both the CO and O atoms are adsorbed on the surface, they move about if they fail to react in the first collision and statistically have a much higher chance of interacting subsequently with a neighbor to successfully overcome the reaction barrier and form CO_2.[60] We note here that the L-R mechanism would be single-shot, while the E-R mechanism would likely have a higher probability of undergoing a productive collision than the L-R mechanism, as the physisorbed species in the E-R mechanism can move about on/near the chemisorbed species, which increases the likelihood of an interaction and hence a reaction.

In a subsequent study by a different group (using DFT, isotope-switch experiments, and *in situ* spectroscopy),[61] another factor was also identified that could potentially lower the activation barrier significantly for the L-H pathway and help explain its dominance over the E-R pathway for CO oxidation over Pt (111) under realistic conditions: CO-assisted activation of $O_{2(g)}$ on the catalyst surface. In this study,[61] the authors reported activated surface molecular oxygen (O_2*) as the kinetically relevant species instead of the surface atomic oxygen species (O*) from dissociative adsorption of O_2 on the catalyst's surface, and they showed that the reaction of activated surface molecular O_2 with CO led to a significantly lower reaction barrier in the L-H pathway.[61]

Although DFT studies are sometimes criticized for incongruences with experimental work, recent studies on coupling DFT energetics with microkinetic models are promising.[62] Microkinetic modeling enables connecting atomistic scale energetics (from DFT) with experimental microscopic and macroscopic information about the reaction system such as the reaction rate (or turnover frequency), flux carrying pathways/selectivity, most abundant surface intermediates, and rate-determining steps.[63] Importantly, microkinetic models can offer a robust complement to DFT studies as no *a priori* assumptions are made regarding the mechanism; thus, there is less onus on the modeler to make accurate simplifying assumptions about the surface chemistry.[62,63] Therefore, we recommend the use of microkinetic models (stochastic ones using kinetic Monte Carlo are more accurate and hence more desirable than mean-field microkinetic models) coupled with DFT studies to ensure that the calculations are performed under experimentally relevant conditions, such as the surface coverage of intermediates,[64] to obtain accurate initial estimates of kinetic and thermodynamic parameters and to achieve quantitative agreement with the experimental results including turnover frequencies, product selectivity, etc.

A second common criticism of DFT-based studies is regarding the configurational choice for the surface active sites, especially when experimental data are not available to guide the modeling effort. However, recent studies have reported a methodology that alleviates some of the errors associated with making such a choice: coupling DFT with *ab initio* molecular dynamics (aiMD) simulations.[6,65] This methodology uses aiMD to sample various local minima structures in given constraints (moles N, pressure P, temperature T, volume V. The idea is that sufficient kinetic energy is available in the system, usually representative of experimental conditions, to transition from one energy minimum to another enabling sampling of various possible states. Typically, such aiMD simulations are run on the order of 10^3 fs with each calculation step on the order of 1 fs to ensure a sufficiently large sampling set. A full aiMD simulation in turn yields various low energy configurations, which can then further be geometrically optimized using periodic DFT to reach the lowest energy configuration among the set of lowest energy configurations identified in aiMD. These low energy configurations of the possible active sites can then be plotted in the phase space of various low energy configurations, some of which may be similar in energy to each other, as a function of temperature and chemical potential of the reactants. Based on the lowest values of the free energy of formation, such a phase space analysis enables the modeler to identify the most thermodynamically probable configuration of the active site(s) under reaction relevant conditions and reduces arbitrariness associated with active site configuration choice otherwise. Briefly, DFT-coupled aiMD and microkinetic modeling are promising methodologies to gain useful and reliable insights regarding the operating surface reaction mechanism in a heterogeneous catalyst.

3.4.1. Limitations. Two major limitations of DFT modeling include the following: (i) the computational time and resources required, as the computational time scales with the system size (N) as N^3-N^5 depending on the exact type of calculation, functional used, presence of heavy elements, mesh size, etc.[66] Comprehensive modeling approaches, such as VASP-DFT, DFT-aiMD, microkinetic modeling, etc., usually require user time at state-of-the-art high performance computing centers around the world, and standalone personal computers cannot be used effectively. Even then, computationally expensive but more accurate functionals can become unfeasible for large systems (>200−300 atoms) or systems requiring explicit treatment of solvent molecules in the condensed phase, etc.[66] (ii) The intrinsic inaccuracies in DFT-based calculated energetics of surface intermediates and transition states, which are sometimes a consequence of the balance between accuracy vs computational time available. Literature evinces that these errors can be greater than 20 kJ mol^{-1} per adsorbed fragment even with the best DFT "realistic" methods and that they do not cancel from intermediate to intermediate in a reaction energy diagram, as the error direction is random and some values are overestimated while others are underestimated.[67,68] Such comparative studies show that the accuracy and precision of various functionals for the computed energies (e.g., for a an adsorbate) can vary from one step to another in a single catalytic cycle, making the choice of optimal functional harder.[67,68]

4. CONCLUSIONS

According to Michel Boudart:[19]

To understand (catalyst) activity at a molecular level or to build a catalytic reactor on an industrial scale, the first necessary information is the turnover frequency and its variation with process variables, temperature, total pressure, and composition. This variation is described by a rate equation. To obtain the latter is an art based on the principle of chemical kinetics.

Thus, an accurate understanding regarding surface mechanisms and reaction rates is at the very heart of catalysis research. Accordingly, the aim of this Perspective is to refresh interest in research on generating accurate insights into the operable reaction mechanism in heterogeneous catalysis. We stress that we are not contending against the existence of any of the well-established reaction mechanisms but are instead trying to elucidate the need to understand each mechanism, especially the elusive E-R mechanism. Herein, four major reaction classes were identified that typically invoke the E-R mechanism without accounting for the key difference between the E-R and L-R mechanisms: H activation, CO oxidation, esterification of alcohols with acids, and SCR of NO_x with NH_3. Despite the prevalent association of the E-R mechanism with the above four reactions, relevant experimental evidence discussed in each section instead shows that all these reactions occur via the L-H mechanism with nonidealities that would lead to apparent discrepancies by fitting the L-H model to the experimental rate data. We then highlighted practical considerations regarding the following experimental and computational techniques that, in our opinion, can more reliably differentiate between L-H and E-R/L-R mechanisms, especially when nonidealities might be present: carefully designed and conducted differential kinetics (partial pressure sweeps, systematic variation in the surface density of catalytic sites), MBS, STM/STS, isotope-switch experiments, and DFT coupled with aiMD and/or microkinetic modeling. The existence of an E-R or L-R mechanism for conventional heterogeneous catalytic reactions using powdered catalysts, however, is still awaiting confirmation with supporting data.

We hope that this Perspective serves to reinvigorate interest in experimental and computational efforts to accurately ascertain between L-H, E-R, and L-R mechanisms in various heterogeneous catalytic reactions and promote consensus and healthy discourse within the field.

ASSOCIATED CONTENT

Ⓢ Supporting Information

The Supporting Information is available free of charge at https://pubs.acs.org/doi/10.1021/acscatal.4c05188.

Bibliometric analysis of catalysis literature identifying the four reactions discussed in this Perspective in the context of L-H vs E-R vs L-R mechanisms (PDF)

AUTHOR INFORMATION

Corresponding Authors

Daniyal Kiani − *Renewable Resources and Enabling Sciences Center, National Renewable Energy Laboratory, Golden, Colorado 80401, United States;* ⓞ orcid.org/0000-0002-9748-3007; Email: daniyal.kiani@nrel.gov

Israel E. Wachs − *Department of Chemical and Biomolecular Engineering, Lehigh University, Bethlehem, Pennsylvania 18015, United States;* ⓞ orcid.org/0000-0001-5282-128X; Email: iew0@lehigh.edu

Complete contact information is available at:

https://pubs.acs.org/10.1021/acscatal.4c05188

Notes

The authors declare no competing financial interest.

REFERENCES

(1) Prins, R. Eley-Rideal, the Other Mechanism. *Top. Catal.* **2018**, *61* (9−11), 714−721.

(2) Ertl, G. Reactions at well-defined surfaces. *Surf. Sci.* **1994**, *299−300*, 742−754.

(3) Langmuir, I. Part II.—"Heterogeneous reactions". Chemical reactions on surfaces. *Trans. Faraday Soc.* **1922**, *17* (0), 607−620.

(4) Kiani, D.; Sourav, S.; Baltrusaitis, J.; Wachs, I. E. Elucidating the Effects of Mn Promotion on SiO2-Supported Na-Promoted Tungsten Oxide Catalysts for Oxidative Coupling of Methane (OCM). *ACS Catal.* **2021**, *11* (16), 10131−10137.

(5) Kiani, D.; Sourav, S.; Baltrusaitis, J.; Wachs, I. E. Oxidative Coupling of Methane (OCM) by SiO2-Supported Tungsten Oxide Catalysts Promoted with Mn and Na. *ACS Catal.* **2019**, *9* (7), 5912−5928.

(6) Kiani, D.; Sourav, S.; Wachs, I. E.; Baltrusaitis, J. A combined computational and experimental study of methane activation during oxidative coupling of methane (OCM) by surface metal oxide catalysts. *Chemical Science* **2021**, *12* (42), 14143−14158.

(7) Mars, P.; van Krevelen, D. W. Oxidations carried out by means of vanadium oxide catalysts. *Chem. Eng. Sci.* **1954**, *3*, 41−59.

(8) Doornkamp, C.; Ponec, V. The universal character of the Mars and Van Krevelen mechanism. *J. Mol. Catal. A: Chem.* **2000**, *162* (1), 19−32.

(9) Vannice, M. A. An analysis of the Mars-van Krevelen rate expression. *Catal. Today* **2007**, *123* (1), 18−22.

(10) Rideal, E. K. A note on a simple molecular mechanism for heterogeneous catalytic reactions. *Mathematical Proceedings of the Cambridge Philosophical Society* **1939**, *35* (1), 130−132.

(11) Eley, D. D. Mechanisms of hydrogen catalysis. *Quarterly Reviews, Chemical Society* **1949**, *3* (3), 209−225.

(12) Attard, G.; Barnes, C. Surfaces. In *Surfaces*; Oxford University Press, 1998; pp 9−16.

(13) Engel, T.; Ertl, G. Surface residence times and reaction mechanism in the catalytic oxidation of CO on Pd(111). *Chem. Phys. Lett.* **1978**, *54* (1), 95−98.

(14) Rangarajan, S.; Mavrikakis, M. A comparative analysis of different van der Waals treatments for molecular adsorption on the basal plane of 2H-MoS2. *Surf. Sci.* **2023**, *729*, 122226.

(15) Bowker, M. The Role of Precursor States in Adsorption, Surface Reactions and Catalysis. *Top. Catal.* **2016**, *59* (8), 663−670.

(16) Rasmussen, P. B.; Holmblad, P. M.; Christoffersen, H.; Taylor, P. A.; Chorkendorff, I. Dissociative adsorption of hydrogen on Cu(100) at low temperatures. *Surf. Sci.* **1993**, *287−288*, 79−83.

(17) van Eck, N. J.; Waltman, L. Visualizing Bibliometric Networks. In *Measuring Scholarly Impact: Methods and Practice*; Ding, Y.; Rousseau, R., Wolfram, D., Eds.; Springer International Publishing, 2014; p 285−320.

(18) Weller, S. Analysis of kinetic data for heterogeneous reactions. *AIChE J.* **1956**, *2* (1), 59−62.

(19) Boudart, M.; Djéga-Mariadassou, G. In *Kinetics of Heterogeneous Catalytic Reactions*; Princeton University Press, 1984.

(20) Boudart, M. Chapter 7 - Heterogeneous Catalysis. In *Reaction in Condensed Phases*; Eyring, H., Ed.; Academic Press, 1975; p 349−411.

(21) Vannice, M. A. In *Kinetics of Catalytic Reactions*; Springer, 2005.

(22) Kiani, D.; Wachs, I. E. The conundrum of "pair sites" in Langmuir-Hinshelwood reaction kinetics in heterogeneous catalysis. *ACS Catal.* **2024**, *14* (13), 10260−10270.

(23) Zambelli, T.; Wintterlin, J.; Trost, J.; Ertl, G. Identification of the "Active Sites" of a Surface-Catalyzed Reaction. *Science* **1996**, *273* (5282), 1688−1690.

(24) Aslam, R.; Usman, M. R.; Irfan, M. F. A comparative study of LHHW and ER kinetic models for NO oxidation over Co3O4 catalyst. *Journal of Environmental Chemical Engineering* **2016**, *4* (3), 2871−2877.

(25) Shirvani, S.; Ghashghaee, M. Mechanism Discrimination for Bimolecular Reactions: Revisited with a Practical Hydrogenation Case Study. *Physical Chemistry Research* **2017**, *5* (4), 727−736.

(26) Campbell, C. T.; Shi, S.-K.; White, J. Kinetics of oxygen titration by carbon monoxide on rhodium. *J. Phys. Chem.* **1979**, *83* (17), 2255−2259.

(27) Beck, A.; Paunović, V.; van Bokhoven, J. A. Identifying and avoiding dead ends in the characterization of heterogeneous catalysts at the gas-solid interface. *Nature Catalysis* **2023**, *6* (10), 873−884.

(28) Paolucci, C.; Khurana, I.; Parekh, A. A.; Li, S.; Shih, A. J.; Li, H.; Di Iorio, J. R.; Albarracin-Caballero, J. D.; Yezerets, A.; Miller, J. T.; et al. Dynamic multinuclear sites formed by mobilized copper ions in NOx selective catalytic reduction. *Science* **2017**, *357* (6354), 898−903.

(29) Jaegers, N. R.; Lai, J.-K.; He, Y.; Walter, E.; Dixon, D. A.; Vasiliu, M.; Chen, Y.; Wang, C.; Hu, M. Y.; Mueller, K. T.; et al. Mechanism by which Tungsten Oxide Promotes the Activity of Supported V2O5/TiO2 Catalysts for NOX Abatement: Structural Effects Revealed by 51V MAS NMR Spectroscopy. *Angew. Chem., Int. Ed.* **2019**, *58* (36), 12609−12616.

(30) Seufitelli, G. V. S.; Park, J. J. W.; Tran, P. N.; Dichiara, A.; Resende, F. L. P.; Gustafson, R. Kinetics of ethylene oligomerization over Ni-H-Beta catalysts. *J. Catal.* **2021**, *401*, 40−53.

(31) Cossee, P. Ziegler-Natta catalysis, I. Mechanism of polymerization of α-olefins with Ziegler-Natta catalysts. *J. Catal.* **1964**, *3* (1), 80−88.

(32) Arlman, E. J. Ziegler-Natta catalysis II. Surface structure of layer-lattice transition metal chlorides. *J. Catal.* **1964**, *3* (1), 89−98.

(33) Marberger, A.; Ferri, D.; Elsener, M.; Kröcher, O. The Significance of Lewis Acid Sites for the Selective Catalytic Reduction of Nitric Oxide on Vanadium-Based Catalysts. *Angew. Chem., Int. Ed.* **2016**, *55* (39), 11989−11994.

(34) Ertl, G. Catalysis is a kinetic phenomenon: The legacy of Michel Boudart. *J. Catal.* **2021**, *404*, 985−986.

(35) Vogt, C.; Weckhuysen, B. M. The concept of active site in heterogeneous catalysis. *Nature Reviews Chemistry* **2022**, *6* (2), 89−111.

(36) Zaera, F. Use of molecular beams for kinetic measurements of chemical reactions on solid surfaces. *Surf. Sci. Rep.* **2017**, *72* (2), 59−104.

(37) Campbell, C. T.; Shi, S.-K.; White, J. M. The Langmuir-Hinshelwood reaction between oxygen and CO on Rh. *Applications of Surface Science* **1979**, *2* (3), 382−396.

(38) Engel, T.; Ertl, G. A molecular beam investigation of the catalytic oxidation of CO on Pd (111). *J. Chem. Phys.* **1978**, *69* (3), 1267−1281.

(39) Ertl, G. Scattering of atomic and molecular beams at metal surfaces. *Surf. Sci.* **1979**, *89* (1), 525−539.

(40) Campbell, C. T.; Ertl, G.; Kuipers, H.; Segner, J. A molecular beam study of the catalytic oxidation of CO on a Pt(111) surface. *J. Chem. Phys.* **1980**, *73* (11), 5862−5873.

(41) Campbell, C. T.; Ertl, G.; Segner, J. A molecular beam study on the interaction of NO with a Pt(111) surface. *Surf. Sci.* **1982**, *115* (2), 309−322.

(42) Rettner, C. T.; Auerbach, D. J. Distinguishing the Direct and Indirect Products of a Gas-Surface Reaction. *Science* **1994**, *263* (5145), 365−367.

(43) Peden, C. H. F.; Herman, G. S.; Z Ismagilov, I.; Kay, B. D.; Henderson, M. A.; Kim, Y.-J.; Chambers, S. A. Model catalyst studies with single crystals and epitaxial thin oxide films. *Catal. Today* **1999**, *51* (3-4), 513−519.

(44) Wachs, I. E.; Madix, R. J. The kinetics and mechanism of catalytic reactions by molecular beam relaxation spectroscopy: HCOOH decomposition. *Surf. Sci.* **1977**, *65* (1), 287−313.

(45) Wachs, I. E.; Madix, R. J. MBRS measurements of overlayer effects on surface lifetimes and reaction probabilities. *J. Catal.* **1980**, *61* (2), 310−315.

(46) Vang, R. T.; Lauritsen, J. V.; Lægsgaard, E.; Besenbacher, F. Scanning tunneling microscopy as a tool to study catalytically relevant model systems. *Chem. Soc. Rev.* **2008**, *37* (10), 2191−2203.

(47) Mansurov, V.; Malin, T.; Teys, S.; Atuchin, V.; Milakhin, D.; Zhuravlev, K. STM/STS Study of the Density of States and Contrast Behavior at the Boundary between (7×7)N and (8×8) Structures in the SiN/Si(111) System. *Crystals* **2022**, *12* (12), 1707.

(48) Zhao, A.; Tan, S.; Li, B.; Wang, B.; Yang, J.; Hou, J. G. STM tip-assisted single molecule chemistry. *Phys. Chem. Chem. Phys.* **2013**, *15* (30), 12428−12441.

(49) Wintterlin, J. Scanning tunneling microscopy studies of catalytic reactions. *Adv. Catal.* **2000**, *45*, 131−206, DOI: 10.1016/S0360-0564(02)45014-6.

(50) Tersoff, J.; Hamann, D. R. Theory of the scanning tunneling microscope. *Phys. Rev. B* **1985**, *31* (2), 805−813.

(51) Rasmussen, P. B.; Hendriksen, B. L. M.; Zeijlemaker, H.; Ficke, H. G.; Frenken, J. W. M. The "Reactor STM": A scanning tunneling microscope for investigation of catalytic surfaces at semi-industrial reaction conditions. *Rev. Sci. Instrum.* **1998**, *69* (11), 3879−3884.

(52) Frenken, J.; Hendriksen, B. The Reactor-STM: A Real-Space Probe for Operando Nanocatalysis. *MRS Bull.* **2007**, *32* (12), 1015−1021.

(53) Hallmark, V. M.; Chiang, S.; Rabolt, J. F.; Swalen, J. D.; Wilson, R. J. Observation of Atomic Corrugation on Au(111) by Scanning Tunneling Microscopy. *Phys. Rev. Lett.* **1987**, *59* (25), 2879−2882.

(54) Wintterlin, J.; Völkening, S.; Janssens, T. V. W.; Zambelli, T.; Ertl, G. Atomic and Macroscopic Reaction Rates of a Surface-Catalyzed Reaction. *Science* **1997**, *278* (5345), 1931−1934.

(55) Park, G. B.; Kitsopoulos, T. N.; Borodin, D.; Golibrzuch, K.; Neugebohren, J.; Auerbach, D. J.; Campbell, C. T.; Wodtke, A. M. The kinetics of elementary thermal reactions in heterogeneous catalysis. *Nature Reviews Chemistry* **2019**, *3* (12), 723−732.

(56) Koster, R.; van der Linden, B.; Poels, E.; Bliek, A. The Mechanism of the Gas-Phase Esterification of Acetic Acid and Ethanol over MCM-41. *J. Catal.* **2001**, *204* (2), 333−338.

(57) Shannon, S. L.; Goodwin, J. G., Jr Characterization of Catalytic Surfaces by Isotopic-Transient Kinetics during Steady-State Reaction. *Chem. Rev.* **1995**, *95* (3), 677−695.

(58) Jehng, J.-M.; Wachs, I. E.; Patience, G. S.; Dai, Y.-M. Experimental methods in chemical engineering: Temperature programmed surface reaction spectroscopy—TPSR. *Canadian Journal of Chemical Engineering* **2021**, *99* (2), 423−434.

(59) Campbell, C. T.; Mao, Z. Analysis and prediction of reaction kinetics using the degree of rate control. *J. Catal.* **2021**, *404*, 647−660.

(60) Baxter, R. J.; Hu, P. Insight into why the Langmuir-Hinshelwood mechanism is generally preferred. *J. Chem. Phys.* **2002**, *116* (11), 4379−4381.

(61) Allian, A. D.; Takanabe, K.; Fujdala, K. L.; Hao, X.; Truex, T. J.; Cai, J.; Buda, C.; Neurock, M.; Iglesia, E. Chemisorption of CO and mechanism of CO oxidation on supported platinum nanoclusters. *J. Am. Chem. Soc.* **2011**, *133* (12), 4498−4517.

(62) Bhandari, S.; Rangarajan, S.; Mavrikakis, M. Combining Computational Modeling with Reaction Kinetics Experiments for Elucidating the In Situ Nature of the Active Site in Catalysis. *Acc. Chem. Res.* **2020**, *53* (9), 1893−1904.

(63) Tian, H.; Rangarajan, S. Microkinetic modeling for heterogeneous catalysis: methods and illustrative applications. In *Catalysis: Volume 34*; Spivey, J., Han, Y.-F., Shekhawat, D., Eds.; The Royal Society of Chemistry, 2022; Vol. *34*, p 56−83.

(64) Bhandari, S.; Rangarajan, S.; Maravelias, C. T.; Dumesic, J. A.; Mavrikakis, M. Reaction Mechanism of Vapor-Phase Formic Acid Decomposition over Platinum Catalysts: DFT, Reaction Kinetics Experiments, and Microkinetic Modeling. *ACS Catal.* **2020**, *10* (7), 4112−4126.

(65) Li, G.; Vollmer, I.; Liu, C.; Gascon, J.; Pidko, E. A. Structure and Reactivity of the Mo/ZSM-5 Dehydroaromatization Catalyst: An Operando Computational Study. *ACS Catal.* **2019**, *9* (9), 8731−8737.

(66) Bursch, M.; Mewes, J.-M.; Hansen, A.; Grimme, S. Best-Practice DFT Protocols for Basic Molecular Computational Chemistry. *Angew. Chem., Int. Ed.* **2022**, *61* (42), No. e202205735.

(67) Hensley, A. J. R.; Ghale, K.; Rieg, C.; Dang, T.; Anderst, E.; Studt, F.; Campbell, C. T.; McEwen, J.-S.; Xu, Y. DFT-Based Method for More Accurate Adsorption Energies: An Adaptive Sum of Energies from RPBE and vdW Density Functionals. *J. Phys. Chem. C* **2017**, *121* (9), 4937−4945.

(68) Wellendorff, J.; Silbaugh, T. L.; Garcia-Pintos, D.; Nørskov, J. K.; Bligaard, T.; Studt, F.; Campbell, C. T. A benchmark database for adsorption bond energies to transition metal surfaces and comparison to selected DFT functionals. *Surf. Sci.* **2015**, *640*, 36−44.